

The long-term effect of radio sources on the ICM

J.F. Basson,^{*} P. Alexander^{*}

Cavendish Astrophysics, Madingley Road, Cambridge CB3 0HE

29 October 2018

ABSTRACT

We have performed 3D hydrodynamical simulations of FR-II radio sources in β -profile cooling-flow clusters. The effects of cooling of the cluster gas were incorporated into a modified version of the ZEUS-MP code. The simulations followed not only the active phase of the radio source, but also the long term behaviour for up to 2 Gyr after the jets of the radio source were switched off. We find as expected that the radio source has a significant effect on the cooling flow while it is active, however we also find that the effects of the radio source on the cluster are long-lived. A buoyancy driven convective flow is established as the remnants of the radio source rise through the cluster dragging material from the cluster core. Although the central Mpc of the cluster reverts to having a cooling flow, this asymmetric convective flow is able to remove the cool gas accumulating at the cluster core and indeed there is a net outflow persisting for timescales of about an order of magnitude longer than the time for which the source is active or longer. The convective flow may also provide a mechanism to enhance the metallicity of the cluster gas at large cluster radii.

Key words: hydrodynamics – galaxies: active – galaxies: jets – X-rays: galaxies : ICM – galaxies: cooling flows

1 INTRODUCTION

There has been significant recent interest in the interaction between radio sources and clusters. This has been driven by observations with both the *ROSAT* and *CHANDRA* satellites which have demonstrated clearly that the presence of a powerful FR-II radio source very significantly affects the ICM/IGM in the vicinity of the source. For example, for the best studied cases of Cygnus A (Carilli, Perley & Harris 1994; Smith et al. 2002) and 3C84 in Perseus (Fabian et al. 2000; Fabian et al. 2002), cavities in the X-ray emitting gas coincident with the radio cocoon are clearly observed and for Cygnus A the effects of a strong bow shock can be clearly seen. Recent reviews of the X-ray observational data on radio-source/cluster interactions are given in McNamara (2002) and McNamara et al. (2000). This interaction between the radio source and the ICM has led a number of authors to consider whether radio sources could solve the so-called “cooling-flow problem” (e.g. Binney & Tabor 1995; McNamara et al. 2000; Reynolds, Heinz & Begelman 2001; Churazov et al. 2001; Quilis, Bower & Balogh 2001; Bohringer et al. 2002; Ruszkowski & Begelman 2002; Brighenti & Mathews 2002a; Reynolds, Heinz & Begelman 2002, hereafter RHB), in which the cool gas expected to ac-

cumulate at the cluster centre as a result of cooling is not detected.

A number of authors have discussed the heating of the ICM by radio sources in the context of the overall energy budget for the cluster (e.g. Binney & Tabor 1995; Kaiser & Alexander 1999; RHB; Alexander 2002 and references therein). Churazov et al. (2002) discuss the energy balance between the cooling flow and the AGN on the basis that there is some feedback between the cooling flow (which results in matter accreting onto a supermassive black hole) and the resulting mechanical power of the AGN. This could also be responsible for the intermittency of the radio source as inferred in some observations (McNamara et al. 2000; Fabian et al. 2000; Owen & Eilek 1998). The energy input from powerful FR-II radio sources is certainly sufficient to have a significant effect on the cluster, however the lifetimes of FR-II radio sources are of order 100 Myr (e.g. Alexander & Leahy 1987), they are therefore transient events in the lifetime of a cooling flow (Fabian 1994). An important question is therefore whether a radio source can have a long-term effect on the cluster; for this reason it is necessary to consider the evolution of the remnants of dead radio sources (i.e. after the jets cease energy injection into the lobes). During these latter stages of evolution the dynamics of the remnants of the radio source will be dominated by buoyancy forces (Gull & Northover 1973). A number of studies have considered the evolution of buoyant plasma bubbles within a cluster. For example Sarazin, Baum & Odea (1995) and Churazov

^{*} Email: j.basson@mrao.cam.ac.uk
p.alexander@mrao.cam.ac.uk

et al. (2001) developed models for 2A 0335+096 and M87 respectively where the observed radio and X-ray structures are modelled by buoyant bubbles of radio-emitting plasma which drag colder material that had been deposited by the cooling flow outwards from the cluster core. These bubbles are Rayleigh-Taylor unstable and therefore form a mushroom cloud type structure (Brüggen & Kaiser 2001). Saxton, Sutherland & Bicknell (2001) have modelled the northern middle radio lobe of Centaurus A as a buoyant bubble, and simulations of buoyant gas in a cluster environment have been presented in 3D by Brüggen et al. (2002) and in high resolution 2D by Brüggen & Kaiser (2002). In all of these studies gas was injected continuously near to the centre of the cluster with zero velocity and in pressure balance with the surrounding gas and the system allowed to evolve. Recently RHB have used a more realistic model which involved setting up the initial radio plasma by simulating a jet; these conditions were then used as the starting point of a new simulation in which the jet activity was turned off.

Although the basic physical processes have been established by these studies, the details of the hydrodynamical evolution of a cooling flow cluster containing a radio source needs to be fully determined if we are to answer the question about the long-term effects of radio sources. In this and a future paper we extend these studies. We follow RHB in simulating a radio source evolving in a cluster so that the initial conditions are as realistic as is possible, however we use a fully 3D simulation and also include cooling of the ICM. The radio source evolves into a cluster environment with an established cooling flow, it is then turned off after a simulation time corresponding to approximately 50 Myr and we then follow the evolution of the system for a further 2 Gyr.

2 COMPUTATIONAL APPROACH

The simulation strategy was designed to model a radio-source event in a cooling-flow cluster atmosphere. The simulations presented here differ from those of RHB in two important respects. Firstly they are fully three dimensional and secondly we include cooling of the cluster gas within an initial cooling flow atmosphere. The ZEUS-MP code (Stone & Norman 1992a,b; Stone, Mihalas & Norman 1992; Norman 2000) with an additional cooling term was used, and the simulations were performed in spherical polar coordinates (r, θ, ϕ) with a grid size of $192 \times 64 \times 64$. The grid spacing was linear in r and ϕ , and ratioed in θ . For a ratioed grid, the size of a grid spacing is a constant multiple of the adjacent grid spacing. A grid structure that is more closely packed along the jet axis (the z -axis in these simulations) can therefore be achieved (RHB).

The cluster atmosphere was modelled by assuming an initial isothermal gas distribution that followed a β -profile $\rho_{\text{ICM}}(r) = \rho_0 / [1 + (r/r_0)^2]^{3\beta/2}$, where r_0 is the core radius. The gravitational potential is dominated by the dark matter and the form of the dark matter potential well was chosen so that the gas was initially in hydrostatic equilibrium. The self-gravity of the gas was ignored resulting in a significant reduction in computational time.

Cooling of the cluster gas was implemented by adding a cooling term to the energy equation, and using a com-

Table 1. Simulation parameters.

Simulation	\dot{M} [$M_{\odot}\text{yr}^{-1}$]	M	n_{ICM} [m^{-3}]	$P_{\text{jet}}/P_{\text{cf}}$
run 1	8.50	100	10^3	291
run 2	996	100	10^4	73

posite cooling curve for the ICM taken from the literature (Sutherland & Dopita 1993; Puy, Grenacher & Jetzer 1999; Tegmark et al. 1997) and assuming a metallicity of $\log(N_{\text{Fe}}/N_{\text{H}}) - \log(N_{\text{Fe}}/N_{\text{H}})_{\odot} = -0.5$. The ZEUS-3D code provides some support for cooling, and the routines were used as the basis for our implementation in ZEUS-MP (which is based on ZEUS-3D). In addition to replacing the original cooling function with the improved version discussed above, the numerical accuracy of the routine was improved. The energy equation including cooling is an implicit differential equation which is solved in the original ZEUS code using an iterative Newton-Raphson (NR) technique. Our modification is to include an additional robust bisection technique to obtain a better initial estimate for the solution in those cases where the initial NR converged slowly – a NR iteration was then performed from this improved initial guess.

The modified code was tested by comparing the results from a simulation with a constant density medium with an analytical solution and by allowing the cooling flow cluster to evolve without the presence of a radio source; the results were in excellent agreement with results in the literature (Sulkanen, Burns & Norman 1989).

The radio source event was simulated by injecting two light anti-parallel conical jets as in RHB. The computational domain is bounded by an inner and outer spherical boundary. At the base of the jet (the inner spherical boundary), outflow conditions are employed except when the jets enter the computational grid, and at the outer boundary, inflow of gas is allowed. The gas injected into the computational domain representing the jet material is subjected to the same cooling as the ICM – this is unphysical since the jet material should cool via synchrotron emission. However the jet material is very low density and its cooling time greatly exceeds the simulation time; therefore the jet material in effect forms a gas with an infinite cooling time.

The parameters characterising the simulations are: the ratio of the jet density to the density of the ICM ($\rho_{\text{jet}}/\rho_{\text{ICM}}$, hereafter ρ_{rat}), the Mach number of the jet with respect to the ICM (M), the steepness and core radius of the cluster gas (β , r_0), the length of time for which the jet is on (t_{on}), and the mass inflow rate of the cluster in the absence of a radio source (\dot{M}) – taken through the spherical surface $r = 300$ kpc at 1 Gyr. The density ratio and Mach number are both defined at the base of the jet. In a forthcoming paper we present an analysis of this parameter space using 2D simulations. Here we discuss two 3D simulations with parameters which represent typical model radio sources, one with a power ratio between the jet and the cooling flow of 291 (run 1), a radio source in a weak cooling flow, and another with a power ratio of 73 (run 2), a radio source in a strong cooling flow. Both simulations have $\beta = 0.5$, $r_0 = 100$ kpc, and $t_{\text{on}} = 59$ Myr. The other parameters are listed in Table 1.

The jets were turned on at $t = 353$ Myr, after a cooling

flow had been established, and they were turned off at $t = 412$ Myr. The simulations ran until a simulation time of $t = 2.4$ Gyr. All simulations were performed on a 16-node Beowulf cluster of 1.3-GHz AMD processors with 512 Mb of memory per node.

3 RESULTS

In Figure 1 we show the time evolution for run 2, the results for run 1 are similar. We shall therefore illustrate our discussion by considering only run 2 and return to compare the results of run 1 and run 2 when we examine the evolution of the cooling flow. Shown in the figure are the density, internal energy (pressure) and velocity structure in the cluster gas and radio source at three different epochs: 401 Myr while the radio source is still active; 518 Myr approximately 100 Myr after the jets have been turned off; 1.89 Gyr an epoch since the jets were switched off which is approximately 25 times the lifetime of the radio source.

3.1 Evolution of the radio remnant and ICM

The evolution of the system while the jets are switched on follows very closely the results from earlier simulations (see for example RHB). In Figure 1 the cocoon is clearly visible as the low density region; the cocoon expands supersonically and is surrounded by a strong bow shock. After the jets are switched off the over-pressured cocoon continues to expand and is preceded still by a bow shock. The expanding remnants soon reach pressure balance, however in this stage they are very light compared to the external gas and rise buoyantly through the cluster. This general behaviour is similar to recent studies by various authors (Churazov et al. 2001; Brüggén & Kaiser 2001; Quilis et al. 2001; Saxton et al. 2001; RHB). Here however as in RHB the initial conditions correspond more realistically to those pertaining to a dead radio source since we have followed the initial evolution when the jets are active and as shown by Alexander (2002) this active phase results in a substantial amount of gas being dragged from the centre of the cluster by the expanding source. The long-term interaction between the buoyantly rising remnants and the cluster is an interplay between the remnants continuing to drag gas out of the cluster and inflow driven both by the cluster gas infilling between the remnants and continued cooling within the cluster.

In Figure 2 we plot the integrated X-ray luminosity and temperature in the cluster gas for run 2 at two epochs after the jets have been switched off.

We shall now consider the evolution of the buoyant phase in a little more detail. Initially the buoyant remnants are surrounded by a weak bow shock. The simulated X-ray emission (Figure 2) is reminiscent of the images recently obtained by *CHANDRA* of radio sources in cooling flow clusters (e.g. Perseus Fabian et al. 2000; Fabian et al. 2002; and A2052/3C317 Rizza et al. 2000; Blanton et al. 2001). In Figure 2b we show the emissivity-weighted temperature integrated along the line of sight. Immediately behind the bow shock the temperature is higher than the surrounding gas, however the temperature of the gas decreases systematically from behind the shock towards the contact surface

with the remnant radio lobe. This cooling is discussed in detail in Alexander (2002) and results from adiabatic cooling of the swept-up ICM as it is dragged out of the cluster core. Simulations and analytical results presented by Brighenti & Mathews (2002b) support the formation of cool gas by expansion. The region occupied by the radio-emitting plasma here appears saturated in the grey-scale.

At long times (after approximately 700 Myr) two main shocks are established within the ICM, which we shall refer to as the leading and trailing shocks (see Figure 1). The leading shock is again a weak bow shock generated by the buoyantly rising remnants, while the trailing shock is produced by infalling ICM. The temperature structure is now particularly interesting. The ICM is heated slightly by the weak bow shock but then cools until the trailing shock; the infalling gas is then heated by the trailing shock and within the cluster core there is little variation in temperature except in regions associated with the radio source remnants themselves. The buoyant remnants undergo substantial mixing with the ICM as they rise through the cluster. A shell of mixed ICM/radio plasma forms with a core of cooler ICM material (Figure 1 and Figure 2d) which is being dragged by the remnants out of the centre of the cluster (see the velocity structure in Figure 1). The buoyant remnant is unstable to large scale instabilities and in these simulations a large part of the remnant is shed at approximately 2 Gyr.

The results presented here are in broad agreement with the studies of buoyant radio plasma presented by a number of authors (Churazov et al. 2001; Brüggén & Kaiser 2001; Quilis et al. 2001; Bohringer et al. 2002; Saxton et al. 2001), however our results differ in important details which are due to the initial conditions we establish by following the evolution of a radio source through its active phase.

3.2 Mass flow and heating in the cluster

In this Section we consider in detail the effect of the radio source on the cooling flow. As pointed out by RHB approximately half the energy input by the radio source goes directly into heating the cluster gas. This is a consequence of the self-similar nature of the expansion. The stored energy of the radio source is just proportional to $p_c V_c$, while the work done by the radio source on the ICM is $\int p_c dV_s$, where subscripts c and s refer to the cocoon and shocked ICM respectively and we make use of the fact that the shocked ICM is approximately at constant pressure and equal to the pressure within the cocoon. For the case of self-similar expansion $V_s \propto V_c$ and V_c and p_c have a power-law dependence on time (Kaiser & Alexander 1997). Hence the stored energy in the cocoon and the energy input to the ICM are proportional at all times and since the volume of the shocked gas is comparable to that of the cocoon the constant of proportionality is approximately unity. Clearly therefore over the lifetime of the source sufficient energy is input to significantly affect the cluster as has been noted by many authors (e.g. Binney & Tabor 1995; Churazov et al. 2001; Brüggén & Kaiser 2001; Quilis et al. 2001; RHB; Alexander 2002). The results presented here demonstrate that it is not only the heating but also the redistribution of mass within the cluster which is important in determining its evolution; this enables the effects of a radio source event to affect a cooling flow on

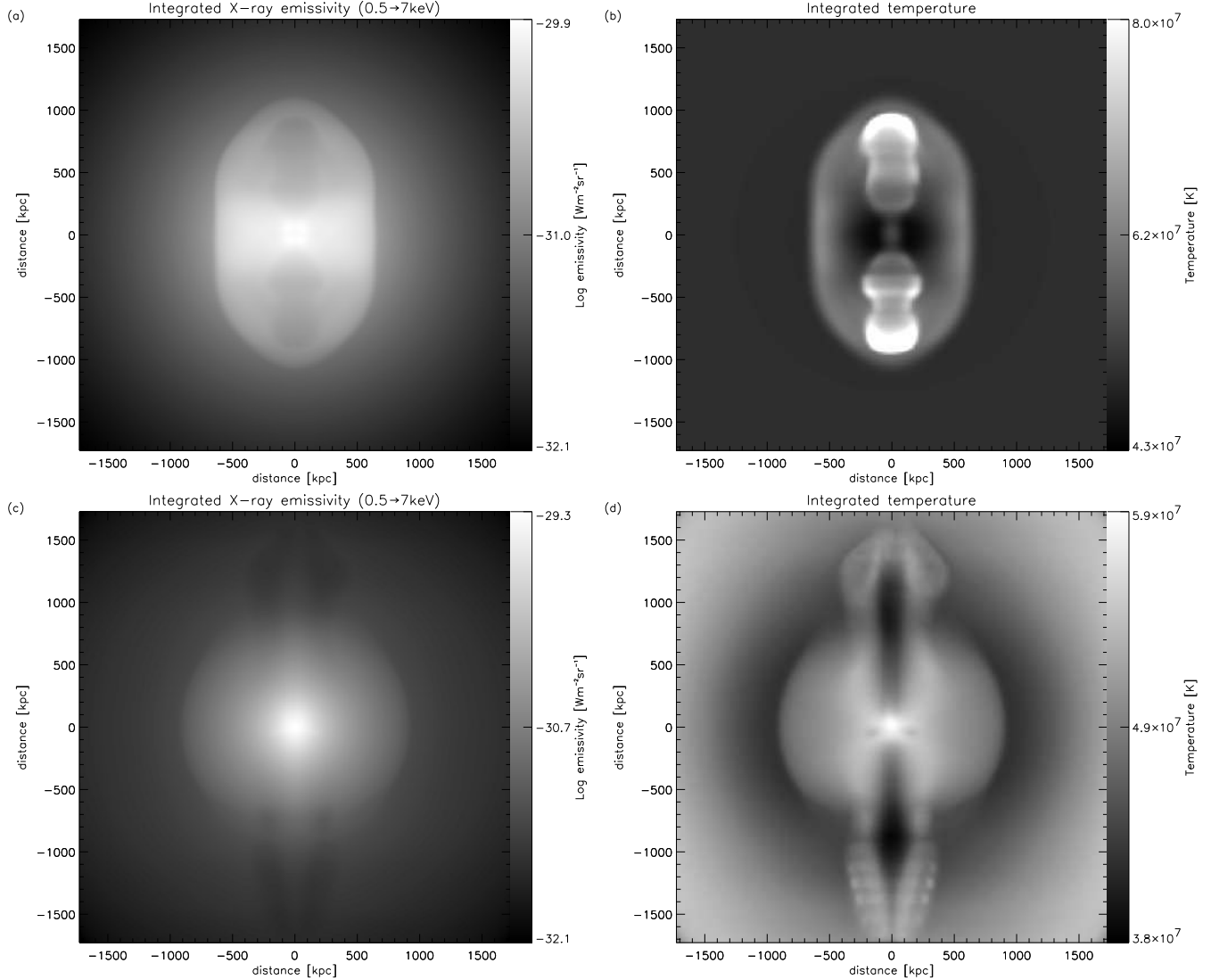


Figure 2. Integrated X-ray luminosity ($\iint \varepsilon_\nu d\nu dl$; $\varepsilon_\nu \propto n^2 T^{-1/2} e^{-h\nu/kT}$ Wm⁻³sr⁻¹Hz⁻¹) between 0.5 and 7 keV and emissivity weighted temperature ($\frac{\int T \varepsilon_\nu dl}{\int \varepsilon_\nu dl}$) at 3 keV for run 2 at 707 Myr ((a) and (b) respectively), and at 2.1 Gyr ((c) and (d)).

timescales very long compared to the period over which the jet is active.

In order to quantify this effect we calculate the net radial mass flow and cumulative flow through a spherical surface of radius 300 kpc. The results for runs 1 and 2 are shown in Figure 3. The flow rate can be divided into 4 stages. Stage 1 is the cooling flow stage when the gas is flowing steadily inwards ($0 \rightarrow 380$ Myr). This is followed by a sharp increase in gas flowing outwards as the shocked ICM and then the cocoon material moves through the surface (380 Myr \rightarrow 520 Myr). The third stage is a sharp increase in gas flowing inwards, here the flow is dominated by the gas that lies between the leading and trailing shocks which is moving towards the centre of the cluster (520 Myr \rightarrow 940 Myr). The final stage depends on the relative powers of the radio source and cooling flow: for the lower power ratio of run 2 there is a return to cooling dominated inflow (> 1.5 Gyr), although the inflow rate remains significantly less than for the same cluster without a radio-source

event; for the higher power ratio of run 1 there is always a net outflow up until the end of the simulation (approximately 2.4 Gyr). Similar behaviour exists for other surfaces with of course different time evolution.

The long-term behaviour of run 2 is particularly interesting. It is clear from Figure 1 that even on these timescales the cluster is very asymmetric. Perpendicular to the original axis of the radio source there is cooling driven inflow. However, the buoyant remnants even at times exceeding 1 Gyr are accompanied by a substantial wake of cluster gas which is moving away from the cluster core. For the strong radio source this outward flow in the cluster gas exceeds the inwards cooling flow. Despite a cooling flow existing in most of the volume of the inner Mpc of the cluster, the asymmetric flow (a remnant of the earlier radio source event) ensures there is no accumulation of cold gas at the cluster core. In these simulations the cooler gas is associated with the buoyant remnant at significant cluster radii. The cluster now contains a large-scale buoyancy driven convective flow.

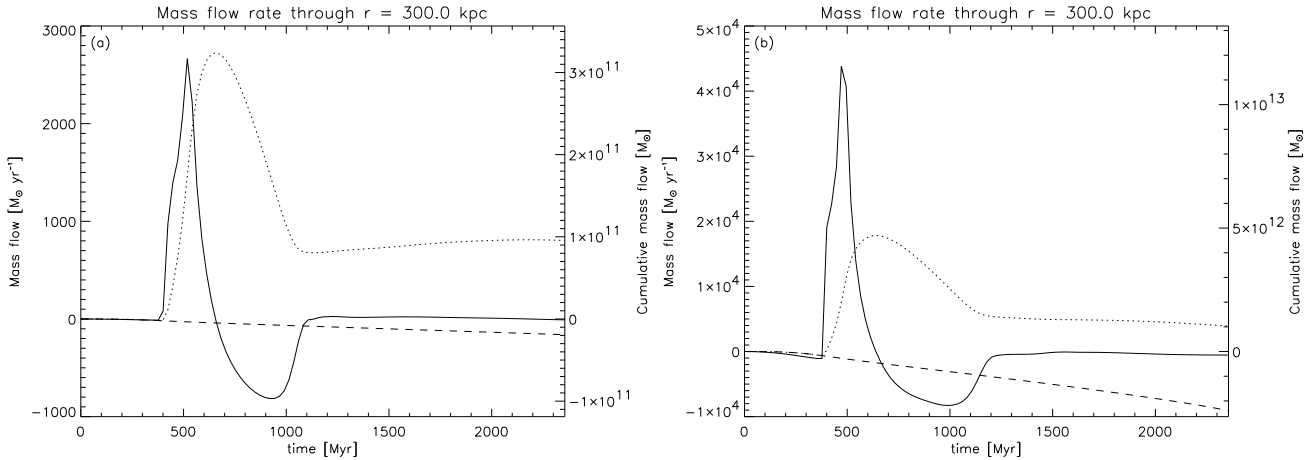


Figure 3. Mass flow ($\oint \rho \mathbf{v} \cdot d\mathbf{A}$) through the sphere $r = 300$ kpc for run 1 (a) and run 2 (b). The solid line (values on left y-axis) is the instantaneous flow rate, and the dotted line (values on right y-axis) is the cumulative flow ($\int \oint \rho \mathbf{v} \cdot d\mathbf{A} dt$). The dashed line is the cumulative flow for the cluster in the absence of a radio source.

4 DISCUSSION

As has been noted by many authors (e.g. Alexander 2002 and references therein; RHB), radio sources are certainly sufficiently energetic to provide substantial heating to a cluster. For example Perseus has an X-ray luminosity of approximately 10^{37} W and powerful radio sources have jet kinetic powers of order 10^{39} W, therefore if the radio source lasts for a few 10^7 yr the energy input from a single powerful radio source is sufficient to provide all the energy to power the X-ray emission for a substantial fraction of a Hubble time. However radio sources are short-lived events and it is necessary to consider more carefully the balance between heating rate and cooling rate.

Our results go some way to understanding the possible role of radio sources in cooling-flow clusters. Our simulations have shown that the effect of a powerful radio source on its host cluster is to modify the dynamics of the cluster gas on timescales very much longer than the lifetime of the active phase of the radio source. The buoyant remnants of the radio source drive a large scale convective flow which is efficient at removing gas from the cluster core on timescales comparable to a Hubble time. By this mechanism the coolest gas will be moved to larger cluster radii. Such a flow would also provide a mechanism for metal enrichment of the cluster gas on large scales.

Observational support for these processes comes from the *CHANDRA* study of A133 (Fujita et al. 2002); this cooling-flow cluster contains a “radio relic” which is connected to the host CD galaxy by a tongue of cooler X-ray emitting gas. The authors consider the possibility that the X-ray structure is explained by uplifting by the buoyant radio relic and demonstrate that this is feasible. They reject this possibility since the morphology of the cool X-ray emission does not agree with the model predictions of Churazov et al. (2001) or Brüggén et al. (2002). However, our simulations predict a structure in the cooler X-ray gas (Figure 2 a&c) which is remarkably similar to the *CHANDRA* results. The structure in the X-ray emitting gas depends strongly on the relative power of the radio source and this will be explored in a forthcoming paper.

The simulations presented here although addressing the same problem as RHB provide important new insight into the evolution of radio-source containing clusters. Firstly the buoyant remnants in the current simulations show less mixing than in the simulations by RHB; the result is that more of the available energy goes into large-scale motion establishing the buoyancy-driven convective flow we have described. This is due in part to our simulations being 3D which permit non-axisymmetric Kelvin Helmholtz instabilities to develop which reduces the amount of mixing although we do see large-scale instabilities. Unfortunately the price we pay for going to 3D is to loose resolution which will suppress high spatial frequency instabilities which would be efficient at mixing. However it is possible that such modes may be suppressed in the real astrophysical system by the magnetic fields which must be present within the radio lobes.

The low grid resolution used here means that numerical diffusion could be a problem. Here we argue that such numerical effects are small in comparison with the overall behaviour observed in our simulations. Firstly, we consider the relative importance of numerical diffusion versus cooling by comparing the results of run 2 with a simulation employing the same parameters, but without cooling (run 2a). For run 2a, the cumulative mass flow through a spherical surface at 300 kpc radius was $2.3 \times 10^{12} M_{\odot}$ compared to $1.0 \times 10^{12} M_{\odot}$ for run 2. This value increases with time due to the convective effects of the rising remnants for run 2a, compared with run 2 where this value is decreasing with time as the cooling flow begins to dominate the behaviour. We are therefore confident that the effects observed in the simulation due to cooling are real, and are not being strongly affected out by numerical diffusion of energy out of the computational domain. A further check on the numerical accuracy is to compare results at differing resolutions. In a forthcoming paper we will present a 2D parameter space investigation, and also consider in detail the effects of varying resolutions on the simulations. These results show that the rate of energy loss through numerical diffusion is essentially independent of the resolution used for resolutions in the range $128 \times 64 \rightarrow 512 \times 512$ and overall energy conserva-

tion in our simulations at all resolutions is as good as that of RHB.

ACKNOWLEDGEMENTS

JFB is supported by the Commonwealth Scholarship Commission in the United Kingdom. We thank Helen Brimmer and David Titterton for managing the Beowulf cluster. We also thank Christian Kaiser and Malcolm Longair for helpful discussions, and the referee for helpful comments.

REFERENCES

- Alexander P., 2002, *astro-ph/0204443*
- Alexander P., and Leahy J. P., 1987, *MNRAS*, 225, 1
- Binney J., Tabor G., 1995, *MNRAS*, 276, 663
- Blanton E. L., Sarazin C. L., McNamara B. R., Wise M. W., 2001, *ApJ*, 558, L15
- Böhringer H., Matsushita K., Churazov E., Ikebe Y., Chen Y., 2002, *A&A*, 382, 804
- Brighenti F., Mathews W. G., 2002a, *ApJ*, 573, 542
- Brighenti F., Mathews W. G., 2002b, *ApJ*, 574, L11
- Brüggen M., Kaiser C. R., 2001, *MNRAS*, 325, 676
- Brüggen M., Kaiser C. R., 2002, *Nat*, 418, 301
- Brüggen M., Kaiser C. R., Churazov E., Enßlin T. A., 2002, *MNRAS*, 331, 545
- Carilli C. L., Perley R. A., Harris D. E., 1994, *MNRAS*, 270, 173
- Churazov E., Brüggen M., Kaiser C. R., Böhringer H., Forman W., 2001, *ApJ*, 554, 261
- Churazov E., Sunyaev R., Forman W., Böhringer H., 2002, *MNRAS*, 332, 729
- Fabian A. C., 1994, *ARA&A*, 32, 277
- Fabian A. C., Sanders J. S., Ettori S., Taylor G. B., Allen S. W., Crawford C. S., Iwasawa K., Johnstone R. M., Ogle P. M., 2000, *MNRAS*, 318, L65
- Fabian A. C., Celotti A., Blundell K. M., Kassim N. E., Perley R. A., 2002, *MNRAS*, 331, 369
- Fujita Y., Sarazin C. L., Kempner J. C., Rudnick L., Slee O. B., Roy A. L., Andernach H., Ehle M., 2002, *astro-ph/0204188*
- Gull S. F., Northover K. J. E., 1973, *Nat*, 244, 80
- Kaiser C. R., Alexander P., 1997, *MNRAS*, 286, 215
- Kaiser C. R., Alexander P., 1999, *MNRAS*, 305, 707
- McNamara B. R., Wise M. W., David L. P., Nulsen P. E. J., Sarazin C. L., 2000, in Durret F., Gerbal D. eds., *Constructing the Universe with Clusters of Galaxies*, IAP 2000 meeting, Paris, France, contribution reference 6.6
- McNamara B. R., Wise M., Nulsen P. E. J., David L. P., Sarazin C. L., Bautz M., Markevitch M., Vikhlinin A., Forman W. R., Jones C., Harris D. E., 2000, *ApJL*, 534, L135
- McNamara B. R., 2002, in Vrtilek S., Schlegel E.M., Kuhi L. eds., *X-rays at Sharp Focus: Chandra Science Symposium*
- Norman M. L., 2000, in Arthur J., Brickhouse N., Franco J. eds., *Revista Mexicana de Astronomia y Astrofisica Conference Series Vol. 9*, p. 66
- Owen F. N., Eilek J. A., 1998, *ApJ*, 493, 73
- Puy D., Grenacher L., Jetzer P., 1999, *A&A*, 345, 723
- Quilis V., Bower R. G., Balogh M. L., 2001, *MNRAS*, 328, 1091
- Reynolds C. S., Heinz S., Begelman M. C., 2001, *ApJL*, 549, L179
- Reynolds C. S., Heinz S., Begelman M. C., 2002, *MNRAS*, 332, 271 (RHB)
- Rizza E., Loken C., Bliton M., Roettiger K., Burns J. O., Owen F. N., 2000, *AJ*, 119, 21
- Ruszkowski M., Begelman M. C., 2002, *astro-ph/0207471*
- Sarazin C. L., Baum S. A., O’Dea C. P., 1995, *ApJ*, 451, 125
- Saxton C. J., Sutherland R. S., Bicknell G. V., 2001, *ApJ*, 563, 103
- Smith M. D., Wilson A. S., Arnaud K. A., Terashina Y., Young A.J., 2002, *ApJ*, 565, 195
- Stone J. M., Mihalas D., Norman M. L., 1992, *ApJS*, 80, 819
- Stone J. M., Norman M. L., 1992a, *ApJS*, 80, 753
- Stone J. M., Norman M. L., 1992b, *ApJS*, 80, 791
- Sulkanen M. E., Burns J.O., Norman M. L., 1989, *ApJ*, 344, 604
- Sutherland R. S., Dopita M. A., 1993, *ApJS*, 88, 253
- Tegmark M., Silk J., Rees M. J., Blanchard A., Abel T., Palla F., 1997, *ApJ*, 474, 1

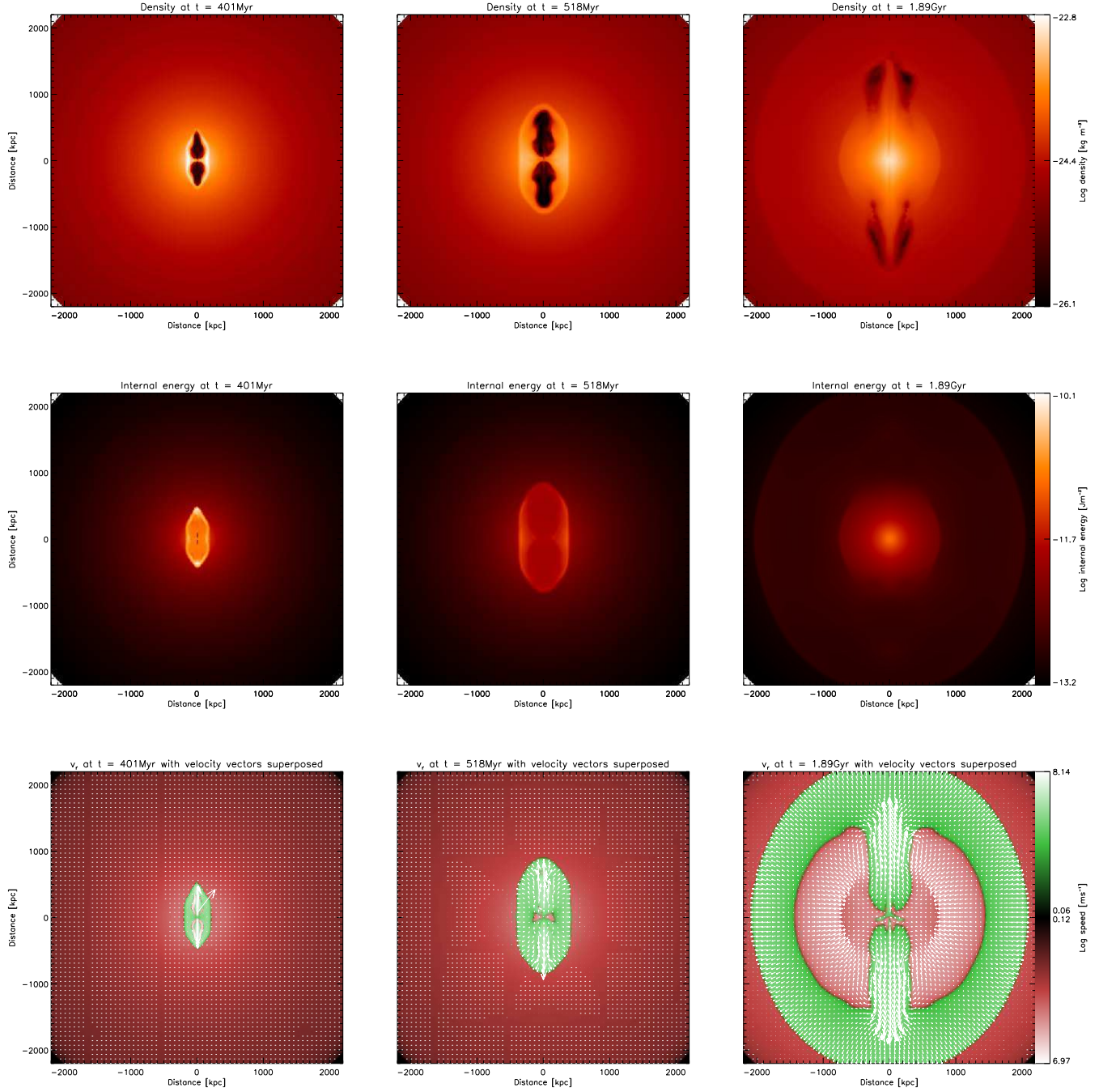


Figure 1. Density, internal energy, and velocity plots (top, middle and bottom rows respectively) at 401 Myr, 518 Myr and 1.89Gyr (left, middle and right columns respectively). The image in the velocity plots is the \hat{r} component of the velocity, with red indicating negative velocity and green positive. The velocity vectors are overlaid.